Mathematical Biosciences and Engineering

MBE, 20(5): 8308–8319.
DOI: 10.3934/mbe.2023363
Received: 26 August 2022
Revised: 09 February 2023
Accepted: 20 February 2023
Published: 01 March 2023

http://www.aimspress.com/journal/MBE

Research article

Machine learning-based evaluation of application value of pulse wave parameter model in the diagnosis of hypertensive disorder in pregnancy

Xinyu Zhang[1], Yu Meng[1], Mei Jiang[2], Lin Yang[1]*, Kuixing Zhang[2,]*, Cuiting Lian[1] and Ziwei Li[1]

[1] Faculty of Environment and Life Sciences, Beijing University of Technology, Beijing 100124, China
[2] College of Intelligence and Information Engineering, Shandong University of Traditional Chinese Medicine, Jinan 250355, China

* **Correspondence:** Email: yanglin@bjut.edu.cn, zhangkuixing@sdutcm.edu.cn; Tel: +8613426181228, +8613789816946.

Abstract: Hypertensive disorder in pregnancy (HDP) remains a major health burden, and it is associated with systemic cardiovascular adaptation. The pulse wave is an important basis for evaluating the status of the human cardiovascular system. This research aims to evaluate the application value of pulse waves in the diagnosis of hypertensive disorder in pregnancy.This research a retrospective study of pregnant women who attended prenatal care and labored at Beijing Haidian District Maternal and Child Health Hospital. We extracted maternal hemodynamic factors and measured the pulse wave of the pregnant women. We developed an HDP predictive model by using support vector machine algorithms at five-gestational-week stages.At five-gestational-week stages, the area under the receiver operating characteristic curve (AUC) of the predictive model with pulse wave parameters was higher than that of the predictive model with hemodynamic factors. The AUC values of the predictive model with pulse wave parameters were 0.77 (95% CI 0.64 to 0.9), 0.83 (95% CI 0.77 to 0.9), 0.85 (95% CI 0.81 to 0.9), 0.93 (95% CI 0.9 to 0.96) and 0.88 (95% CI 0.8 to 0.95) at five-gestational-week stages, respectively. Compared to the predictive models with hemodynamic factors, the predictive model with pulse wave parameters had better prediction effects on HDP.Pulse waves had good predictive effects for HDP and provided appropriate guidance and a basis for non-invasive detection of HDP.

Keywords: hypertensive disorders in pregnancy; pulse wave parameters; hemodynamic factors; support vector machine; predictive model

1. Introduction

Hypertensive disorders in pregnancy (HDP) are pregnancy-specific systematic disorders that globally affect 5–10% of all pregnancies[1–4]. HDP is a major cause of maternal and fetal mortality and morbidity worldwide, and it is important to make an accurate prediction of HDP to improving maternal and infant outcomes [5–8].

Pregnancy is accompanied by a change in the hemodynamic environment. During normal pregnancy, the cardiac output (CO), heart rate, and intravascular volume increase, which decreases the total peripheral resistance (TPR) and blood pressure [9–13]. The main physiological manifestation of HDP is systemic small vessel spasms, which result in increased TPR and blood pressure and reduced cardiac output in pregnant women [14–16]. Therefore, HDP can be predicted by a combination of multiple indicators of maternal hemodynamic factors [17,18], but some of the hemodynamic factors are obtained through invasive means, which could cause discomfort to the pregnant woman. Pulse waves originate from the rhythmic contraction and diastole of the heart, form at the root of the aorta and then propagate rapidly along the arterial tree to the peripheral vasculature with a constant reflex, making them rich in cardiovascular information about the human body and a powerful predictor of future cardiovascular events. Previous studies have shown that pulse wave parameters are an important basis for evaluating the physiological and pathological status of the human cardiovascular system [19,20]. The morphological parameters can reflect the cardiac ejection fraction and vascular elasticity. The presystolic wave can reflect the physiological phenomenon of the process from atrial systolic depolarization to ventricular systolic depolarization. By decomposing the pulse wave by applying a fourth-order Gaussian, the fourth Gaussian parameter can locate the presystolic wave [21]. The descending branch of the pulse wave is related to the peripheral resistance and vascular elasticity of the body, and it better reflects the hemodynamic information of the body [22]. The current research mainly focuses on exploring the value of morphological parameters in HDP. However, the application value of other parameters to HDP remains unclear.

In this study, we extracted the waveform morphology parameters, Gaussian decomposition parameters, and descending branch energy parameters of the pulse wave. We used support vector machine algorithms to establish HDP predictive models based on hemodynamic factors and pulse wave parameters, respectively. The predictive effects of the models were compared to investigate the predictive value of the pulse wave on HDP and to provide a possibility for the non-invasive monitoring of HDP.

2. Materials and methods

2.1. Subjects

We performed a retrospective study on pregnant women who attended prenatal checkups at Beijing Haidian District Maternal and Child Health Hospital from 2015 to 2016. We excluded women with the following conditions: (a) long-term drug use; (b) fetal malformations; (c) suffering from

chronic hypertension, diabetes or other cardiovascular diseases. A total of 168 pregnant women were included in this study, 49 of whom had HDP and 119 who were healthy pregnant women

2.2. Data acquisition

We collected maternal demographic information, blood pressure, TPR, CO, and mean arterial pressure (MAP) data from the hospital's electronic medical record. Beginning the first maternity examination of the pregnant women, the radial artery pulse wave waveform of each pregnant woman was collected and tracked.

Before testing, pregnant women were asked to remain quiet for 5 minutes. A pressure transducer was placed above their left radial artery and the recordings were captured via a Power Lab data acquisition system (ADInstruments Pty., Ltd., Power Lab 8/35, Bella Vista NSW 2153, Australia) at a rate of 1000 Hz. We repeated the sampling three times for each person and then took the average value. In the end, a total of 1269 pulse waves were obtained from the HDP group and 4160 pulse waves were obtained from the control group. As shown in Figure 1, to facilitate the calculation of feature points, we normalized the sampling points and amplitude of each pulse waveform to 0–100.

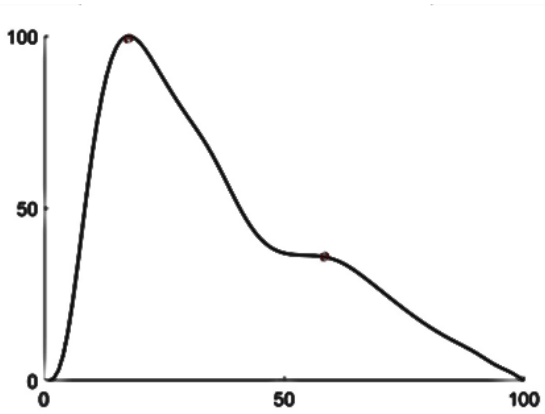

Figure 1. Normalized radial artery pulse waveform.

2.3. Feature extraction of pulse wave

In this study, three main types of features of pulse waveforms were extracted: waveform morphology parameters, Gaussian decomposition parameters [23], and descending branch energy parameters.

The pulse wave contained three main waveform components: main wave, tidal wave, and dicrotic wave. As shown in Figure 2, A is the main wave peak point, B is the tidal wave peak point, C is the dicrotic wave peak point, M is the pulse wave endpoint, N_A is the main wave peak point location, N_B is the tidal wave peak point location, N_C is the dicrotic wave peak point location, P_A is the main wave amplitude, P_B is the tidal wave amplitude, and P_C is the dicrotic wave amplitude. We extracted the position parameters (N_A, N_B, N_C), amplitude parameters (P_A, P_B, P_C), position difference parameters ($N_{B\text{-}A}=N_B-N_A$; $N_{C\text{-}A}=N_C-N_A$) and amplitude ratio parameters ($P_{B/A}=P_B/P_A$; $P_{C/A}=P_C/P_A$) of the three main waveform components.

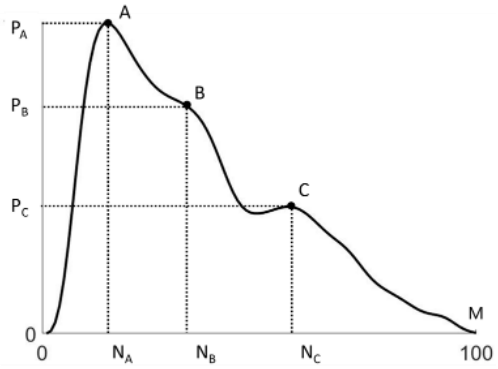

Figure 2. Morphological parameters of the pulse wave.

For the acquisition of the Gaussian parameters, we used four Gaussian functions to decompose the pulse wave, as shown in Figure 3. The Gaussian equation is as follows:

$$f_i(t) = \sum_{i=1}^{4} H_i * e^{-\frac{2(t-T_i)^2}{W_i^2}}, \tag{2.1}$$

where H_i (i=1,2,3,4) denotes the amplitude of each Gaussian waveform, T_i (i=1,2,3,4) denotes the position of each Gaussian wave peak, and W_i (i=1,2,3,4) denotes the width of each Gaussian wave.

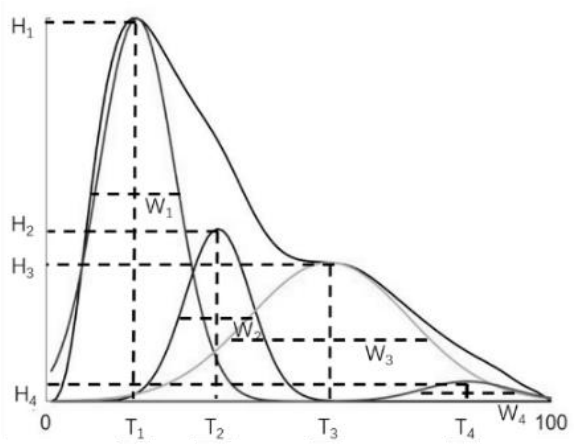

Figure 3. Gaussian decomposition graph of the pulse wave.

We extracted the descending branch energy parameters of the pulse wave, which included the waveform slope parameters, the area ratio parameters and the waveform descending branch complexity parameters. For the waveform slope parameters, we extracted the slope of the peak point to the endpoint (SL_A, SL_B, SL_C, SL_D), the slope between the peak points (SL_1, SL_2) and the slope ratio ($SL_{2/1}$) as slope parameters. We calculated the area under the curve line and the area under the line between the peak point and the endpoint, and we used the ratio between the two areas as the area ratio parameters (Dr_1, Dr_2, Dr_3). We extracted the sample entropy of the waveform ($SampEn_{AM}$) between the peak point of the main wave and the endpoint as the complexity parameter. The parameters can be

calculated as follows:

$$SL_A=\frac{P_A}{(100-N_A)} \tag{2.2}$$

$$SL_B=\frac{P_B}{(100-N_B)} \tag{2.3}$$

$$SL_C=\frac{P_C}{(100-N_C)} \tag{2.4}$$

$$SL_D=\frac{P_D}{(100-N_D)} \tag{2.5}$$

$$SL_1=\frac{P_A-P_B}{(N_B-N_A)} \tag{2.6}$$

$$SL_2=\frac{P_A-P_C}{(N_C-N_A)} \tag{2.7}$$

$$SL_{2/1}=\frac{SL_2}{SL_1} \tag{2.8}$$

$$Dr_1=\frac{0.5*P_A*(100-N_A)-S_{AM}}{0.5*P_A*(100-N_A)} \tag{2.9}$$

$$Dr_2=\frac{0.5*P_B*(100-N_B)-S_{BM}}{0.5*P_B*(100-N_B)} \tag{2.10}$$

$$Dr_3=\frac{0.5*P_C*(100-N_C)-S_{CM}}{0.5*P_C*(100-N_C)} \tag{2.11}$$

where S_{AM} is the area under the waveform line from waveform point A to point M, S_{BM} is the area under the waveform line from waveform point B to point M, and S_{CM} is the area under the waveform line from waveform point C to point M.

2.4. Statistical analysis

Statistical analysis of the characteristic parameters was performed using SPSS Statistics (version 26.0, IBM, Inc.). We performed independent sample t-tests for characteristics between the HDP and control groups and selected factors with $P<0.05$, and the parameter values are expressed as the X (mean) ± SD (standard deviation). In this paper, the data were characterized by a large variety of parameters and the data volume was small, so we choose the support vector machine algorithm to build the predictive model with hemodynamic factors and pulse wave parameters, respectively. A model for the prediction of HDP was constructed by using MATLAB (R2019b, MathWorks, Inc.), and the model evaluation parameters included the area under the ROC curve (AUC), accuracy, sensitivity, and specificity.

2.5. Ethical approval

The studies were approved by the Ethics Committee of Science and Technology of Beijing University of Technology.

3. Results

3.1. Baseline characteristics

In this research, 168 women were included. We compared the basic information of the pregnant women in the HDP and control groups. We found that there were no statistically significant differences in age and height, and that HDP pregnant women had a significantly higher pre-pregnancy body mass index than the control group (P<0.05). The gestational age of delivery of those with HDP was significantly lower than that of the control group. The basic information is shown in Table 1.

Table1. Comparison of basic information on HDP group and control group.

Factor	HDP group	Control group
Age (years)	30.08 ± 3.83	30.16 ± 3.85
Height (cm)	162.1 ± 4.88	162.03 ± 5.29
Pre-BMI	24.35 ± 4.56*	21.34 ± 2.26
Gestational week of delivery (weeks)	37.88 ± 1.87*	39.01 ± 1.05

Note: *P<0.05. Pre-BMI, pre-pregnancy body mass index.

3.2. Model construction results

We compared the differences in CO, TPR, systolic blood pressure (SBP), diastolic blood pressure (DBP), and MAP between the HDP group and control group during pregnancy. As shown in Table 2, significant differences in the CO and TPR between the HDP and control groups at 35–40 weeks (P < 0.05). The SBP, DBP, and MAP of the HDP group and control group showed significant differences after the 14th week (P < 0.05). As shown in Table 3, all pulse wave parameters, except W_4, were significantly different in at least one gestational week stage (P<0.05).

We used SVMs to build the predictive models with hemodynamic factors and pulse wave parameters, respectively. As shown in Table 4, we found that the AUC of the predictive model with hemodynamic factors was between 0.5 and 0.6, and the prediction effects were not good. The AUC of the predictive model with pulse wave parameters was higher than that of the predictive model with hemodynamic factors at the same stage. As shown in Table 4 and Figure 1, the prediction effects of the model with pulse wave parameters were poor in the first trimester, but the AUC was higher than 0.8 after 14 weeks, and the prediction effect was good. The predictive model with pulse wave parameters had the best prediction effects at 28–34 weeks (ROC-AUC = 0.93, accuracy = 84.86%, PR-AUC = 0.91).

Table 2. Comparison of CO, TPR, SBP, DBP and MAP during pregnancy between HDP group and control group.

Factor	Group	0–13 weeks	14–20 weeks	21–27 weeks	28–34 weeks	35–40 weeks
CO	Control	2.68±0.71	3.02±0.93	2.65±0.67	2.7±0.69	2.67±0.75
	HDP	2.73±0.79	2.73±0.86	2.52±0.71	2.64±0.67	2.41±0.81*
TPR	Control	1.4±0.39	1.18±0.40	1.24±0.40	1.18±0.38	1.23±0.46
	HDP	1.36±0.43	1.3±0.34	1.31±0.34	1.22±0.34	1.45±0.45*
SBP	Control	115.03±10.55	112.1±9.18	107.11±9.88	106.45±9.61	111.5±10.47
	HDP	118.38±8.83	120.14±8.83*	114.68±10.09*	116.83±8.16*	122.5±15.19*
DBP	Control	73.45±8.25	68.66±7.46	67.14±7.82	66.3±7.46	69.81±8.11
	HDP	75±8.14	75.49±9.57*	73.78±9.23*	73.45±7.31*	79.57±12.67*
Map	Control	90.78±8.87	85.94±7.14	83.12±8.48	82.11±7.84	86.43±8.68
	HDP	93.02±8.40	93.78±9.45*	90.38±9.53*	90.7±7.19*	97.35±12.89*

Note: * $P<0.05$ compared to Control

Table 3. Comparison of pulse wave parameters during pregnancy between HDP group and control group.

Factor	Group	0–13 weeks	14–20 weeks	21–27 weeks	28–34 weeks	35–40 weeks
N_A	Control	15.84±2.74	17.26±1.98	17.8±1.92	17.78±2.15	18.09±2.02
	HDP	16.6±2.70*	18.37±2.19*	17.88±2.13	17.33±2.02*	17.71±2.30*
N_B	Control	31.08±4.01	33.17±2.91	33.75±2.93	33.56±3.15	33.6±2.94
	HDP	32.26±4.26*	34.91±3.24*	34.33±3.31*	33.13±3.13*	33.48±3.38
N_C	Control	54.25±6.00	59±5.92	59.48±5.61	59.83±6.10	58.75±5.67
	HDP	55.64±6.43*	60.31±6.07*	60.56±5.95*	59.38±7.14	57.71±5.52*
P_B	Control	72.79±7.95	64.87±8.56	63.46±8.16	61.97±8.84	65.05±9.06
	HDP	73.32±10.01	66.21±10.88*	68.07±8.00*	68.33±10.64*	69.05±11.37*
P_C	Control	40.75±8.08	35.94±8.45	35.55±6.62	34.5±6.87	34.86±7.53
	HDP	40.5±12.29	35.39±7.87	35.73±8.03	34.69±7.67	38.05±6.16*
N_{B-A}	Control	15.25±1.59	15.91±1.37	15.96±1.26	15.78±1.39	15.51±1.26
	HDP	15.63±1.73*	16.55±1.48*	16.45±1.50*	15.83±1.44	15.73±1.42
N_{C-A}	Control	38.41±4.35	41.74±4.88	41.68±4.54	42.04±4.95	40.65±4.70
	HDP	39.03±4.50	41.94±5.20	42.68±4.72*	42.05±6.18	39.99±4.53
$P_{B/A}$	Control	0.73±0.08	0.65±0.09	0.63±0.08	0.62±0.09	0.65±0.09
	HDP	0.73±0.10	0.66±0.11*	0.68±0.08*	0.68±0.11*	0.69±0.11*
$P_{C/A}$	Control	0.41±0.08	0.36±0.08	0.36±0.07	0.35±0.07	0.35±0.08
	HDP	0.41±0.12	0.35±0.08	0.36±0.08	0.35±0.08	0.38±0.06*
H_1	Control	98.14±3.12	98.9±1.92	99.03±1.36	99.18±1.44	99.53±1.09
	HDP	98.35±1.76	99.38±1.11*	98.84±1.54	98.94±1.62	99.62±1.11
H_2	Control	59.43±10.73	52.13±9.48	48.82±7.95	47.38±9.32	47.62±9.15
	HDP	58.6±9.82	50.81±11.50	54.4±9.69*	53.43±10.56*	52.21±10.36*
H_3	Control	38.77±7.71	34.66±8.23	34.69±6.46	33.57±6.75	33.89±7.34

continue to next page

Factor	Group	0–13 weeks	14–20 weeks	21–27 weeks	28–34 weeks	35–40 weeks
	HDP	38.71±11.18	34.2±7.82	34.72±7.87	33.7±7.20	36.78±6.19*
H_4	Control	8.65±3.77	4.26±3.81	3.22±2.55	3.16±2.73	4.86±3.34
	HDP	6.83±4.19	4.03±3.62	4.29±2.75*	3.87±2.94	5.12±2.65
T_1	Control	15.84±2.74	17.26±1.98	17.8±1.92	17.78±2.15	18.09±2.02
	HDP	16.6±2.70*	18.37±2.19*	17.88±2.13	17.33±2.02*	17.71±2.30*
T_2	Control	31.09±4.00	33.17±2.89	33.75±2.90	33.56±3.14	33.6±2.92
	HDP	32.24±4.23*	34.92±3.23*	34.33±3.29*	33.16±3.09*	33.44±3.37
T_3	Control	54.25±6.00	59±5.92	59.48±5.61	59.83±6.10	58.75±5.67
	HDP	55.64±6.43*	60.31±6.07*	60.56±5.95*	59.38±7.14	57.71±5.52*
T_4	Control	81.07±5.00	79.94±8.46	79.88±8.85	79.45±8.15	82.09±8.65
	HDP	82.25±5.43	79.95±8.62	82.71±6.74*	81.4±7.46*	81.28±6.14
W_1	Control	18.08±3.41	19.76±2.61	20.22±2.53	20.24±2.95	20.46±2.55
	HDP	19.22±3.82*	21.34±2.86*	20.61±2.90*	19.88±2.71*	20.3±3.29
W_2	Control	20.02±2.94	20.73±2.76	20.38±2.31	20.11±2.49	19.2±2.28
	HDP	20.05±2.51	20.7±2.92	20.82±2.58*	20.22±2.80	19.5±2.67
W_3	Control	37.47±5.93	38.57±6.08	40.48±5.72	40.17±5.92	40.95±6.12
	HDP	37.49±5.53	38.95±5.11	40.22±5.43	41.5±5.62*	39.82±5.57*
W_4	Control	26.54±7.56	25.92±10.54	25.98±12.22	26.94±11.04	24.33±10.36
	HDP	25.88±8.55	23.48±11.02	25.05±10.55	24.33±10.74	26.38±8.56
SL_A	Control	1.17±0.04	1.19±0.03	1.2±0.03	1.2±0.03	1.21±0.03
	HDP	1.19±0.04*	1.21±0.03*	1.2±0.03	1.2±0.03*	1.2±0.03*
SL_B	Control	1.04±0.12	0.96±0.12	0.94±0.12	0.92±0.13	0.97±0.13
	HDP	1.07±0.15	1±0.14*	1.02±0.13*	1.01±0.14*	1.03±0.18*
SL_C	Control	0.88±0.16	0.86±0.17	0.86±0.12	0.84±0.15	0.83±0.15
	HDP	0.89±0.23	0.89±0.23	0.89±0.23*	0.89±0.23	0.89±0.23*
SL_D	Control	0.7±0.16	0.77±0.18	0.79±0.17	0.76±0.16	0.8±0.17
	HDP	0.69±0.17	0.81±0.16*	0.83±0.18*	0.8±0.16*	0.8±0.19
SL_1	Control	1.79±0.53	2.22±0.58	2.3±0.55	2.42±0.60	2.27±0.64
	HDP	1.72±0.66	2.03±0.62*	1.96±0.58*	1.99±0.65*	1.97±0.73*
SL_2	Control	1.55±0.20	1.54±0.19	1.55±0.15	1.57±0.18	1.61±0.19
	HDP	1.52±0.26	1.55±0.21	1.51±0.18*	1.57±0.18	1.56±0.18*
$SL_{2/1}$	Control	0.88±0.17	0.69±0.12	0.68±0.14	0.67±0.14	0.72±0.13
	HDP	1±0.27	0.74±0.16*	0.84±0.12*	0.81±0.19*	0.94±0.31*
Dr_1	Control	0.48±0.04	0.48±0.04	0.48±0.03	0.48±0.03	0.48±0.03
	HDP	0.47±0.04	0.47±0.04	0.47±0.03*	0.47±0.03*	0.47±0.03
Dr_2	Control	0.34±0.07	0.41±0.08	0.41±0.07	0.43±0.07	0.41±0.08
	HDP	0.34±0.1	0.39±0.09*	0.39±0.06*	0.4±0.09*	0.37±0.07*
Dr_3	Control	0.53±0.06	0.51±0.07	0.49±0.07	0.49±0.06	0.48±0.06
	HDP	0.53±0.05	0.5±0.07	0.48±0.07*	0.48±0.06*	0.5±0.07*
$SampEn_{AM}$	Control	0.07±0.01	0.06±0.02	0.06±0.02	0.06±0.03	0.06±0.02
	HDP	0.07±0.02	0.06±0.02	0.06±0.02*	0.06±0.02	0.06±0.02

Note: * $P<0.05$ compared to Control

Table 4. Test results of the models.

Gestational weeks	Model	AUC	accuracy	Sensitivity	Specificity
0–13 weeks	Hemodynamic	0.62[0.45,0.78]	65.44%	61.52%	52.30%
	Pulse wave	0.67[0.52,0.82]	61.82%	76.92%	68.28%
14–20 weeks	Hemodynamic	0.64[0.45,0.82]	75.51%	88.24%	46.67%
	Pulse wave	0.83[0.77,0.9]	74.83%	79.73%	69.68%
21–27 weeks	Hemodynamic	0.68[0.47,0.89]	57.14%	47.06%	72.73%
	Pulse wave	0.85[0.81,0.9]	76.86%	85.47%	68.80%
28–34 weeks	Hemodynamic	0.70[0.5,0.89]	58.62%	81.25%	30.77%
	Pulse wave	0.93[0.9,0.96]	84.86%	91.15%	78.10%
35–40 weeks	Hemodynamic	0.60[0.39,0.8]	78.75%	86.57%	38.46%
	Pulse wave	0.88[0.8,0.95]	77.00%	64.71%	89.80%

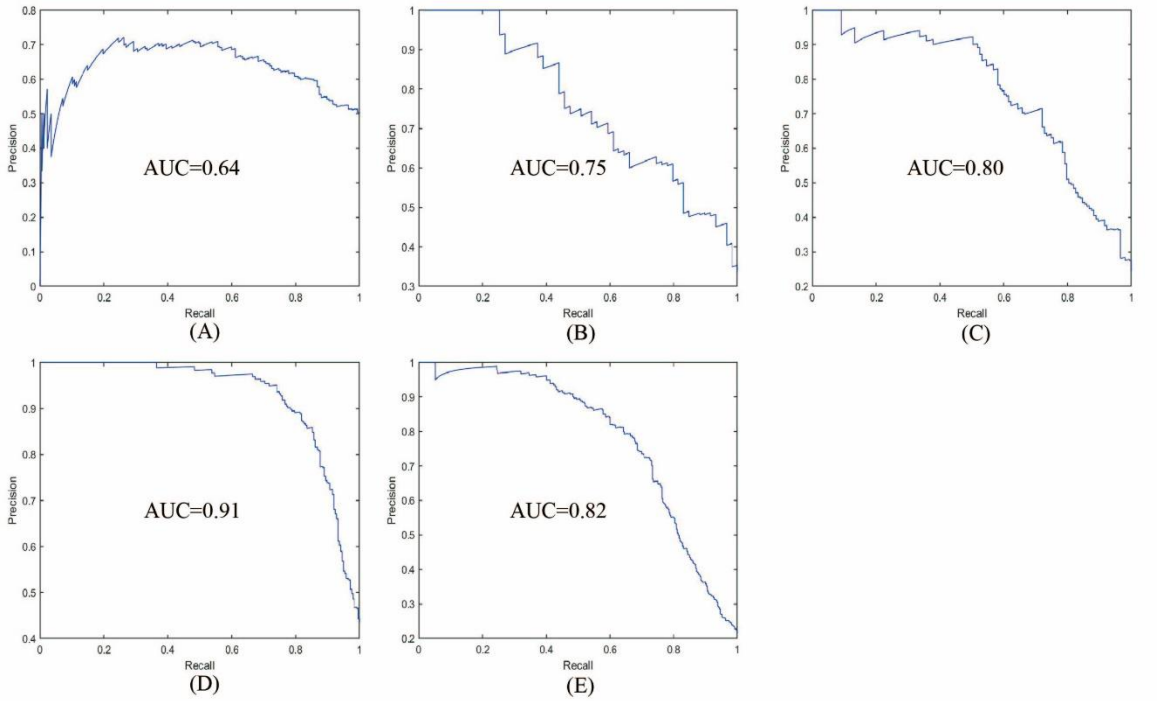

Figure 1. PR curves for the predictive model with pulse wave parameters. (A) PR curve for 0–13 weeks; (B) PR curve for 14–20 weeks; (C) PR curve for 21–27 weeks; (D) PR curve for 28–34 weeks; (E) PR curve for 35–40 weeks.

4. Discussion

HDP are diseases that coexist with pregnancy and hypertension, which are major causes of increased maternal morbidity and mortality. We developed a predictive model with hemodynamic factors and with pulse wave parameters, respectively, and then we compared the prediction effects of the two models. We found that the predictive model with pulse wave parameters outperformed the predictive model with hemodynamic factors.

Blood pressure monitoring has long been used as an important diagnostic tool for prenatal screening [24]. In this study, we found that the SBP and DBP showed significant differences between the HDP and control groups. However, the predictive value of these hemodynamic factors, including the blood pressure, for HDP was not high, which is similar to the findings of Xu et al. [25]. Xu et al. found that hemodynamic parameters were only 77.03% effective in predicting HDP. The pulse wave originates from the rhythmic contraction and diastole of the heart and travels through arterial relationships throughout the body, therefore, the pulse wave contains information about cardiovascular pathologies in the body. Pulse waves were closely related to the cardiovascular physiological state, including waveform amplitude and waveform period and other waveform morphological information, which largely reflected many physiopathological characteristics of the human. In this study, after the 14th week, the AUC of the predictive model with pulse wave parameters was over 80%. Compared to predictive models with hemodynamic factors, we found that the predictive model with pulse wave parameters made better predictinos. We took into account the fact that the number of healthy pregnant women and HDP pregnant women in the data was not 1:1, and we further investigated the results by constructing a Precision-Recall curve. As shown in Figure 1, the PR-AUC after 14 weeks was greater than that from 0–13 weeks, and the PR-AUC was greatest at 28–34 weeks, indicating that the best prediction was achieved at that stage. Both the predictive model with hemodynamic factors and the predictive model with pulse wave parameterspoorly predicted at 0–13 weeks, because a pregnant woman's body has not yet shown any obvious abnormal state in the first trimester.

Finally, there were some limitations in this research. First, this research had a high number of collections from pregnant women, but the total number of pregnant women was not large. The number of pregnant women participating in the study needs to be increased. Second, this study was a retrospective study, and further prospective studies should be added to evaluate and improve the model.

5. Conclusions

We developed HDP predictive models by using hemodynamic factors and pulse wave parameters, respectively, and found that the predictive model with pulse wave parameters had better prediction effects. The pulse wave has a good predictive value for HDP, which provided guidance for the non-invasive detection of HDP and offered the possibility of self-monitoring during pregnancy.

Acknowledgments

This research was funded by the National Key R&D Program of China (2019YFC0119700) and National Natural Science Foundation of China (U20A201163). We would like to thank all participants in this research and the obstetrics staff of Beijing Haidian District Maternal and Child Health Hospital for their work in patient registration.

Conflict of interest

We declare that the research was conducted in the absence of any commercial or financial relationships that could be construed as a potential conflict of interest.

References

1. J. A. Hutcheon, S. Lisonkova, K. S. Joseph, Epidemiology of pre-eclampsia and the other hypertensive disorders of pregnancy, *Best Pract. Res. Clin. Obstet. Gynaecol.*, **25** (2011), 391–403. https://doi.org/10.1016/j.bpobgyn.2011.01.006
2. M. Umesawa, G. Kobashi, Epidemiology of hypertensive disorders in pregnancy: prevalence, risk factors, predictors and prognosis, *Hypertens. Res.*, **40** (2017), 213–220. https://doi.org/10.1038/hr.2016.126
3. V. Mahendra, S. L. Clark, M. S. Suresh, Neuropathophysiology of preeclampsia and eclampsia: A review of cerebral hemodynamic principles in hypertensive disorders of pregnancy, *Pregnancy Hypertens.*, **23** (2021), 104–111. https://doi.org/10.1016/j.preghy.2020.10.013
4. P. Li, T. Xiong, Y. Hu, Hypertensive disorders of pregnancy and risk of asthma in offspring: protocol for a systematic review and meta-analysis, *BMJ Open*, **10** (2020), e035145. http://dx.doi.org/10.1136/bmjopen-2019-035145
5. J. M. Roberts, P. A. August, G. Bakris, J. R. Barton, I. M. Bernstein, M. Druzin, Hypertension in pregnancy, *Obstet. Gynecol.*, **122** (2013), 1122–1131. https://doi.org/10.1097/01.AOG.0000437382.03963.88
6. S. L. Boulet, M. Platner, N. T. Joseph, A. Campbell, R. Williams, K. K. Stanhope, et al., Hypertensive disorders of pregnancy, cesarean delivery, and severe maternal morbidity in an urban safety-net population, *Am. J. Epidemiol.*, **189** (2020), 1502–1511. https://doi.org/10.1093/aje/kwaa135
7. V. D. Garovic, W. M. White, L. Vaughan, M. Saiki, S. Parashuram, O. Garcia-Valencia, et al., Incidence and long-term outcomes of hypertensive disorders of pregnancy, *J. Am. Coll. Cardiol.*, **75** (2020), 2323–2334. https://doi.org/10.1016/j.jacc.2020.03.028
8. P. Wu, C. A. Chew-Graham, A. H. Maas, L. C. Chappell, J. E. Potts, M. Gulati, et al., Temporal Changes in Hypertensive Disorders of Pregnancy and Impact on Cardiovascular and Obstetric Outcomes, *Am. J. Cardiol.*, **125** (2020), 1508–1516. https://doi.org/10.1016/j.amjcard.2020.02.029
9. W. P. Metsaars, W. Ganzevoort, J. M. Karemaker, S. Rang, H. Wolf, Increased sympathetic activity present in early hypertensive pregnancy is not lowered by plasma volume expansion, *Hypertens. Pregnancy*, **25** (2006), 143–157. https://doi.org/10.1080/10641950600912927
10. V. A. Lopes van Balen, J. J. Spaan, C. Ghossein, S. M. van Kuijk, M. E. Spaanderman, L. L. Peeters, Early pregnancy circulatory adaptation and recurrent hypertensive disease: an explorative study, *Reprod. Sci.*, **20** (2013), 1069–1074. https://doi.org/10.1177/1933719112473658
11. O. C. Logue, E. M. George, G. L. Bidwell, Preeclampsia and the brain: neural control of cardiovascular changes during pregnancy and neurological outcomes of preeclampsia, *Clin. Sci.*, **130** (2016), 1417–1434. https://doi.org/10.1042/CS20160108
12. S. Moors, K. J. J. Staaks, M. Westerhuis, L. R. C. Dekker, K. M. J. Verdurmen, S. G. Oei, et al., Heart rate variability in hypertensive pregnancy disorders: A systematic review, *Pregnancy Hypertens.*, **20** (2020), 56–68. https://doi.org/10.1016/j.preghy.2020.03.003
13. J. S. Cnossen, R. K. Morris, G. ter Riet, B. W. Mol, J. A. van der Post, A. Coomarasamy, et al., Use of uterine artery Doppler ultrasonography to predict pre-eclampsia and intrauterine growth restriction: A systematic review and bivariable meta-analysis, *Cmaj*, **178** (2008), 701–711. https://doi.org/10.1503/cmaj.070430

14. I. G. Fabry, T. Richart, X. Chengz, L. M. Van Bortel, J. A. Staessen, Diagnosis and treatment of hypertensive disorders during pregnancy, *Acta Clin. Belg.*, **65** (2010), 229–236. https://doi.org/10.1179/acb.2010.050
15. S. Hale, M. Choate, A. Schonberg, R. Shapiro, G. Badger, I. M. Bernstein, Pulse pressure and arterial compliance prior to pregnancy and the development of complicated hypertension during pregnancy, *Reprod. Sci.*, **17** (2010), 871–877. https://doi.org/10.1177/1933719110376545
16. I. M. Bernstein, S. A. Hale, G. J. Badger, C. A. McBride, Differences in cardiovascular function comparing prior preeclamptics with nulliparous controls, *Pregnancy Hypertens.*, **6** (2016), 320–326. https://doi.org/10.1016/j.preghy.2016.07.001
17. T. Arakaki, J. Hasegawa, M. Nakamura, S. Hamada, M. Muramoto, H. Takita, et al., Prediction of early- and late-onset pregnancy-induced hypertension using placental volume on three-dimensional ultrasound and uterine artery Doppler, *Ultrasound Obst. Gyn.*, **45** (2015), 539–543. https://doi.org/10.1002/uog.14633
18. G. Sun, Q. Xu, S. Zhang, L. Yang, G. Liu, Y. Meng, et al., Predicting hypertensive disorders in pregnancy using multiple methods: Models with the placental growth factor parameter, *Technol. Health Care*, **29** (2021), 427–432. https://doi.org/10.3233/THC-218040
19. A. R. Wang, J. Su, S. Zhang, L. Yang, Radial pulse waveform and parameters in different types of athletes, *Am. J. Transl. Res.*, **8** (2016), 1180–1189.
20. A. Wang, L. Yang, W. Wen, S. Zhang, D. Hao, S. G. Khalid, et al., Quantification of radial arterial pulse characteristics change during exercise and recovery, *J. Physiol. Sci.*, **68** (2018), 113–120. https://doi.org/10.1007/s12576-016-0515-7
21. L. Wang, L. Xu, S. Feng, M. Q. Meng, K. Wang, Multi-Gaussian fitting for pulse waveform using Weighted Least Squares and multi-criteria decision making method, *Comput. Biol. Med.*, **43** (2013), 1661–1672. https://doi.org/10.1016/j.compbiomed.2013.08.004
22. B. Saugel, A. S. Meidert, N. Langwieser, J. Y. Wagner, F. Fassio, A. Hapfelmeier, et al., An autocalibrating algorithm for non-invasive cardiac output determination based on the analysis of an arterial pressure waveform recorded with radial artery applanation tonometry: a proof of concept pilot analysis, *J. Clin. Monit. Comput.*, **28** (2014), 357–362. https://doi.org/10.1007/s10877-013-9540-8
23. K. Li, S. Zhang, L. Yang, H. Jiang, D. Hao, L. Zhang, et al., Gaussian modelling characteristics of peripheral arterial pulse: Difference between measurements from the three trimesters of healthy pregnancy, *J. Healthc. Eng.*, **2018** (2018), 1308419. https://doi.org/10.1155/2018/1308419
24. L. C. Poon, N. A. Kametas, C. Valencia, T. Chelemen, K. H. Nicolaides, Hypertensive disorders in pregnancy: screening by systolic diastolic and mean arterial pressure at 11–13 weeks, *Hypertens. Pregnancy*, **30** (2011), 93–107. https://doi.org/10.3109/10641955.2010.484086
25. Q. Xu, G. Sun, S. Zhang, G. Liu, L. Yang, Y. Meng, et al., Prediction of hypertensive disorders in pregnancy based on placental growth factor, *Technol. Health Care*, **29** (2021), 165–170. https://doi.org/10.3233/THC-218017